Solid State Electronics Letters 2 (2020) 49–54

Contents lists available at ScienceDirect

Solid State Electronics Letters

journal homepage: http://www.keaipublishing.com/en/journals/solid-state-electronics-letters/

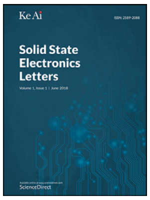

Simulation and analysis of the forward bias current–voltage–temperature characteristics of W/4H-SiC Schottky barrier diodes for temperature-sensing applications

Kamal Zeghdar[a], Hichem Bencherif[a], Lakhdar Dehimi[a,b], Fortunato Pezzimenti[c,*], Francesco G. DellaCorte[c]

[a] LMSM, University of Biskra, BP 145, 07000 Biskra, Algeria
[b] Faculty of Material Science, University of Batna, 05000 Batna, Algeria
[c] DIIES–Mediterranea University, Feo di Vito, Reggio Calabria I-89122, Italy

ARTICLE INFO

Article history:
Received 29 January 2020
Revised 29 April 2020
Accepted 22 August 2020
Available online 12 September 2020

Keywords:
Schottky barrier
Ideality factor
Temperature
Thermionic emission

ABSTRACT

The current-voltage (I_D-V_D) characteristics of W/4H-SiC Schottky barrier diodes (SBDs) are investigated in the 303–448 K temperature range by means of a numerical simulation study. Results showed a good agreement with measurements for a bias current ranging from 100 nA up to 10 mA. The main device parameters, such as the barrier height and ideality factor are found strongly temperature-dependent. The observed behaviours are interpreted by using the thermionic emission (TE) theory with a single Gaussian distribution of the barrier height (BH). The corresponding Richardson constant is $A^* = 148.8$ Acm^{-2}K^{-2}. This value is close to the theoretical one of 146 Acm^{-2}K^{-2} for n-type 4H-SiC.

1. Introduction

Silicon Carbide (SiC) is a promising semiconductor for sensing applications due to its excellent electrical and physical properties [1,2]. The wide bandgap energy and low intrinsic carrier concentration allow SiC-based devices to be functional at high temperatures. The most commonly used metal for Schottky contacts are titanium (Ti) and Nickel (Ni). However, their large-scale diffusion is limited by the high density of defects at the interface and the high temperature of the annealing process [3]. For that reason, Tungsten (W) is considered as a promising candidate for the fabrication of Schottky barrier diodes (SBDs). Starting from the experimental results on Mo/4HSiC SBDs reported in [3], in this paper, the measured I_D-V_D characteristics of W/4H–SiC SBDs are investigated by means of a numerical simulation study in the 303–448 K temperatures range. The temperature dependencies of the current transport parameters are explained with the assumption of the existence of Gaussian distribution of the Schottky barrier around the W/4H–SiC interface.

2. Device structure and simulation models

The schematic cross section of the SBDs considered in this work is shown in Fig. 1. The substrate used for the experimental devices was a n-type 4H–SiC <0001> from Cree Inc. The epi-layer is 10-µm-thick and it has a net doping density of about 1.3×10^{16} cm^{-3}. The diodes have a circular geometry with a diameter of 200 µm.

The Schottky contacts are formed by depositing tungsten through an electron-beam (e-beam) lithography evaporation technique at a pressure of 1×10^{-5} Pa. Then, the annealing process is performed in an open furnace at 500 °C under an N_2 flow of about 1000 sccm. Finally, the backside ohmic contact of the wafer is formed by e-beam deposition of a 250-nm-thick molybdenum film, followed by an

---

[*] Corresponding author.
E-mail address: fortunato.pezzimenti@unirc.it (F. Pezzimenti).

https://doi.org/10.1016/j.ssel.2020.08.001

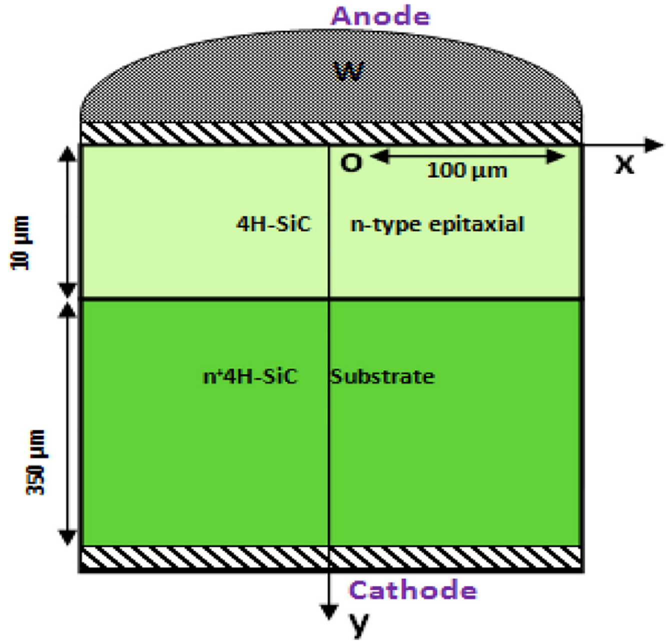

Fig. 1. W/4H-SiC Schottky barrier diode schematic cross section.

Table 1
Physical models and reference parameters.

$R_{SRH}=\dfrac{pn-n_i^2}{\tau_p(n+n_i exp(\frac{E_{trap}}{kT}))+\tau_n(p+n_i exp(-\frac{E_{trap}}{kT}))}$	$n_i = 6.7 \times 10^{-11}$ cm^{-3}
$R_{Auger}=(C_n n+C_p p)(np-n_i^2)$	$C_{An} = 5 \times 10^{-31}$ cm^6/s $C_{Ap} = 2 \times 10^{-31}$ cm^6/s
$\Delta E_{gp,\ n}=A_{p,\ n}\left(\frac{N_{A\ ,}^{-}\ {}^{+}{}_{D}}{10^{18}}\right)^{1/2}+B_{p,n}\left(\frac{N_{A\ ,}^{-}\ {}^{+}{}_{D}}{10^{18}}\right)^{1/3}+C_{p,n}\left(\frac{N_{A\ ,}^{-}\ {}^{+}{}_{D}}{10^{18}}\right)^{1/4}$	$A_p = 1.54 \times 10^{-3}$ $B_p = 1.3 \times 10^{-2}$ $C_p = 1.57 \times 10^{-2}$ $A_n = 1.17 \times 10^{-2}$ $B_n = 1.5 \times 10^{-2}$ $C_n = 1.9 \times 10^{-2}$
$\mu_{n,p}=\mu_{0n,p}^{\min}+\dfrac{\mu_{0n,p}^{\max}-\mu_{0n,\ p}^{\min}}{1+(\frac{N}{N_{n,p}^{crit}})^{\delta_{n.p}}}$ $\mu_{n,p}(E)=\dfrac{\mu_{n,p}}{[1+(E\frac{\mu_{n,p}}{v_{sat}})^{k_{n.p}}]^{\frac{1}{k_{n.p}}}}$	$\mu_{0n}^{\min}$ =40 cm^2/V·s $\mu_{0p}^{\min}$ =15.9 cm^2/V·s $\mu_{0n}^{\max}$ =950 cm^2/V·s $\mu_{0p}^{\max}$ =125 cm^2/V·s $N_n^{crit} = 2 \times 10^{17}$ cm^{-3} $N_p^{crit} = 1.76 \times 10^{19}$cm^{-3} $\delta_n = 0.76$, $\delta_p = 0.34$ $k_n = 2$, $k_p = 1$ $v_{sat} = 2 \times 10^7$ cm/s

annealing treatment at about 1070 °C in a vacuum furnace. Further details about the diode fabrication process are provided in [4], and reference therein.

The numerical simulation analysis was carried out by using the 2D Atlas Silvaco simulator solving the Poisson's equation and the carrier continuity equations onto a finely meshed device structure [5]. The main physical models used during the simulations are summarized in Table 1.

They include the Shockley–Read–Hall and Auger recombination processes [6,7], the apparent band-gap narrowing [8], and the concentration and temperature dependent carrier mobility involving also the high-field effects [9,10]. More in detail, in Table 1, E_{trap} is the difference between the trap energy level and the intrinsic Fermi level, n_i is the intrinsic carrier concentration, τ_n and τ_p are the carrier lifetimes, C_n and C_p are the Auger coefficients, $A_{n,p}$, $B_{n,p}$ and $C_{n,p}$, are appropriate 4H-SiC constants, N is the local concentration of the ionized impurities, v_{sat} is the carrier saturated drift velocity, and $\mu_{0n,p}^{\min}$, $\mu_{0n,p}^{\max}$, $N_{n,p}^{crit}$, $k_{n,p}$, and $\delta_{n,p}$ are specific model parameters.

3. Results and discussion

3.1. I_D-V_D-T characteristics

The measuredand simulated forward I_D-V_D-T curves of the considered W/4H-SiC SBDs for seven different temperatures from 303 K to 448 K are shown in Fig. 2.

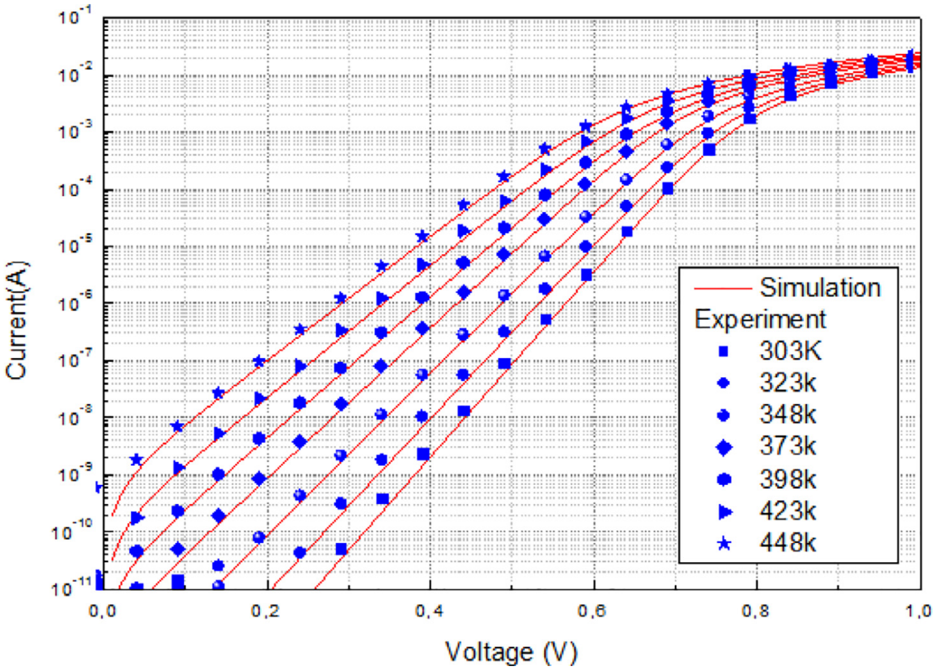

Fig. 2. Measured (symbols) and simulated (solid lines) current–voltage curves of the W/4H-SiC Schottky diode at different temperatures.

The Schottky thermionic emission model accounting for the field-dependent barrier lowering effect was applied in order to fit the experimental curves. It is worth noting that the numerical simulation results are in good agreement with the experimental data. In addition, these results could be further optimized by including the deep trap influence on the recombination processes. For the sake of simplicity, this effect has been neglected in this work.

From Fig. 2, we extracted the fundamental diode parameters, namely the saturation current I0, the Schottky barrier height θ_B, and the ideality factor n. The barrier height and ideality factor are found to be strong temperature dependent. The barrier height and ideality factor are found to be strong temperature dependent. In particular, from the slope of the different straight lines in Fig. 2, by increasing the temperature the ideality factor decreases while θ_B increases. In particular, $n = 1.071$ and $\theta_B = 1.104$ eV at 303 K, and $n = 1.048$ and $\theta_B = 1.164$ eV at 498 K.

The effective Richardson constant (A^*) obtained from the classic Richardson plot is 1.23 A cm−2K−2 that is much lower than the value calculated theoretically which is close to 146 A cm−2K−2 for n-type 4H-SiC [11]. The enormous difference between the theoretical value of A^* and the extracted one from the temperature dependence of the (I_D-V_D-T) characteristics may be explained by the inhomogeneity of the barrier.

3.2. Inhomogeneous barrier analysis

Fig. 3 shows the plot of zero-bias barrier height $\varnothing_{\mathrm{B}}$ versus the ideality factor n.

The extrapolation of $\varnothing_{\mathrm{B}}$ for $n = 1$ gives a homogeneous barrier height of approximately 1.287 eV. The significant increase of $\varnothing_{\mathrm{B}}$ and decrease of n with temperature are possibly caused by the Schottky barrier inhomogeneities, namely some lateral patches of different barrier heights [12,13].

In order to evidence the presence of the barrier inhomogeneity, the temperature dependence of the ideality factor can be reported in the form of a plot of nT vs. T [14]. This behavior for the investigated SBDs is reported in Fig. 4. Here, the dashed line represents the ideal curve ($n = 1$).

The $n(T)$ calculation shows a linear trend, nearly parallel to the straight line relative to the ideal Schottky contact. This result means that the ideality factor can be expressed in the form $n = 1 + T_0/T$ where T_0 is a constant. This behavior, which is commonly referred to the "T_0 anomaly", is typical of a real Schottky contact (with barrier inhomogeneities) [15]. The fit of the experimental data gives $T_0 = 21.47$ K.

The $\varnothing_{\mathrm{B}}$ and n anomalous behaviors reported previously are explained by assuming spatially inhomogeneous barrier heights and potential fluctuations at the Schottky interface that consist of low and high barrier areas. It is assumed that $\bar{\varnothing}_{\mathrm{B}}$ and σ are linearly bias-dependent on Gaussian parameters ($\overline{\varnothing_{\mathrm{B}}} = \bar{\varnothing}_{\mathrm{B0}} + \rho_2 \mathrm{V}$; $\sigma^2 = \sigma_0{}^2 + \rho_3 \mathrm{V}$) [16]. The values obtained for $\bar{\varnothing}_{\mathrm{B0}}$, σ_0, ρ_2, and ρ_3 are 1.286 eV, 97.4 meV, 3.65 mV, and −3.29 mV, respectively. The standard deviation is a measure of the barrier homogeneity where the lower value of $\sigma_0$corresponds to a more homogeneous barrier height.

However, the value of $\sigma_0 = 97.4$ meV is not small if compared to the mean value of $\bar{\varnothing}_{\mathrm{B0}} = 1.286$ eV (7.58%), which indicates the presence of the barrier inhomogeneities. The slope and intercept of the linear fitting of the plot $\ln(\mathrm{I_0}/\mathrm{T}^2) - (\mathrm{q}^2\sigma_0^2/2\mathrm{k}^2\mathrm{T}^2)$ vs. q/kT in Fig. 5 allow to determine $\bar{\varnothing}_{\mathrm{B0}} = 1.287$ eV and $A^* = 148.8$ A $\mathrm{cm}^{-2}\mathrm{K}^{-2}$. These results are in perfect accordance with the expected theoretical value.

Fig. 6 shows the experimental I_D–V_D-T curves together with the ones simulated using the parameters determined from the Gaussian distribution method. As can be seen, an excellent data agreement is achieved.

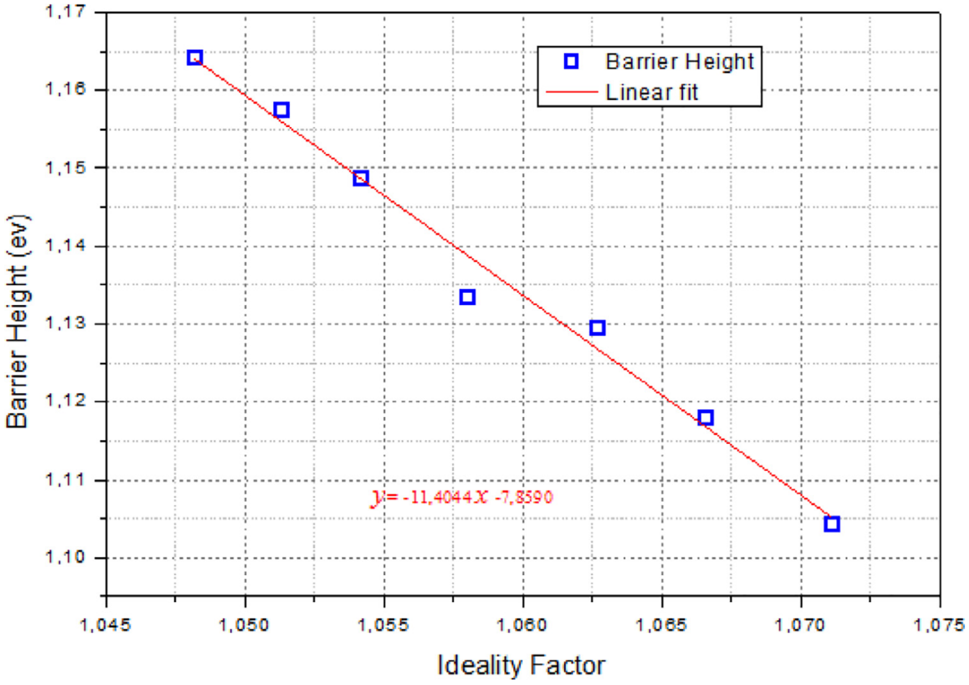

Fig. 3. Zero bias barrier height vs. ideality factor.

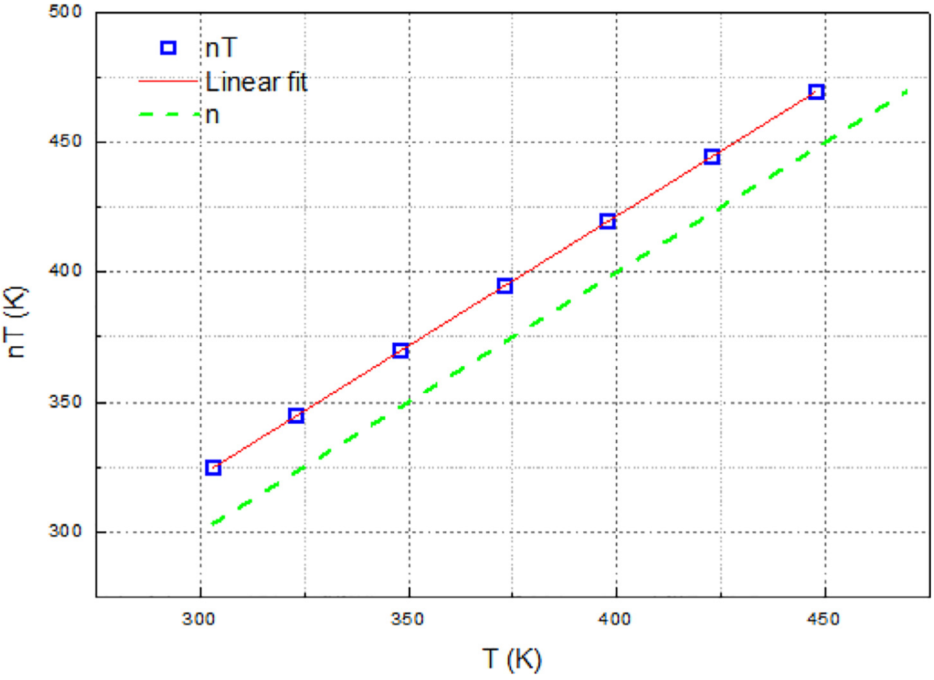

Fig. 4. Plot of nT vs. T showing the T_0 effect.

3.3. Performance as temperature sensor

The performance of the W/4H–SiC SB diode as temperature sensor is evaluated for a fixed bias current by investigating the V_D-T data as shown in Fig. 7.

In particular, for different values of I_D, the diode sensitivity (S) is extracted from the slope of the best linear fit as shown in Fig. 8.

Here, the plot of the coefficient of determination (R^2), which determines the correlation between the measurements to a straight line, is also reported. As we can see, the V_D –T curves show a remarkable degree of linearity and the diode sensitivity increases almost monotonically from 1.28 mV/K up to 2.41 mV/K. Finally, the maximum $R^2 = 0.99961$ is calculated for $I_D = 5.97$ nA, corresponding to $S = 2.33$ mV/K.

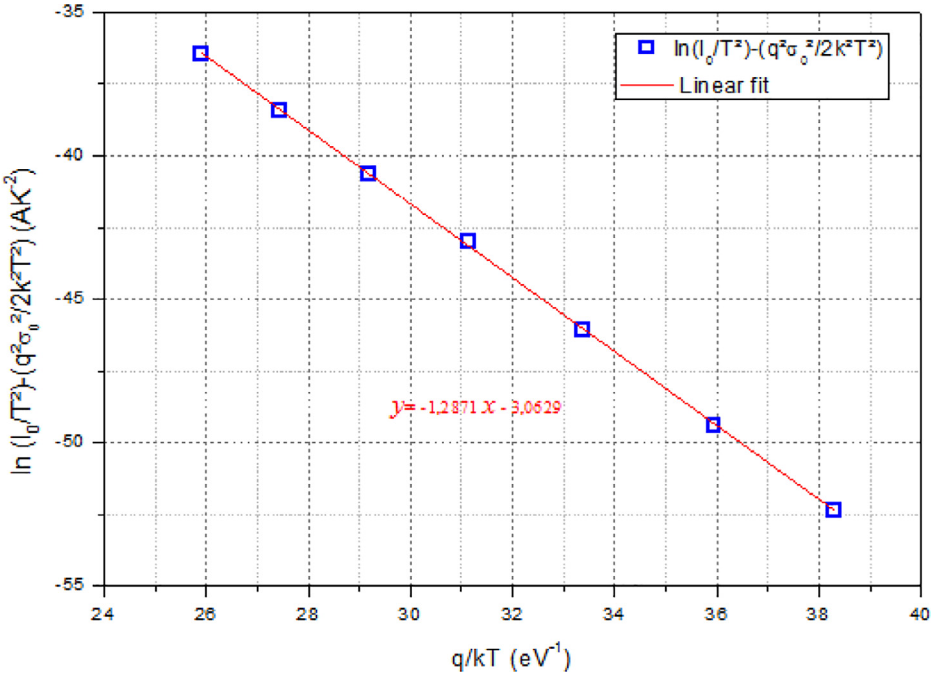

Fig. 5. $ln(I_0/T^2) - (q^2\sigma_0^2/2k^2T^2)$ vs. q/kT.

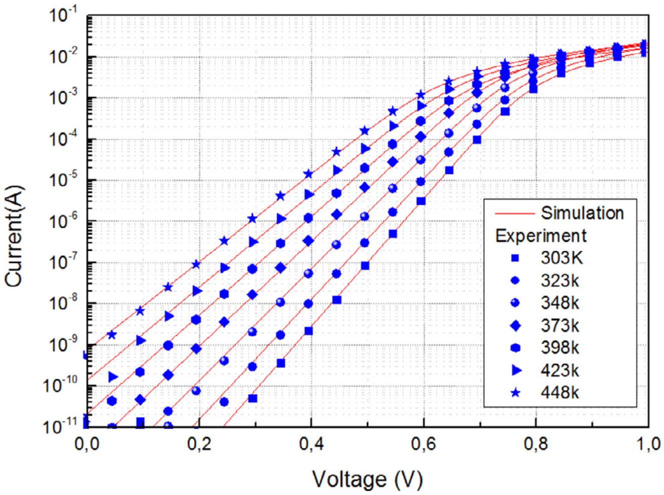

Fig. 6. Experimental and fitted I–V plots at different temperatures by using the Gaussian distribution method.

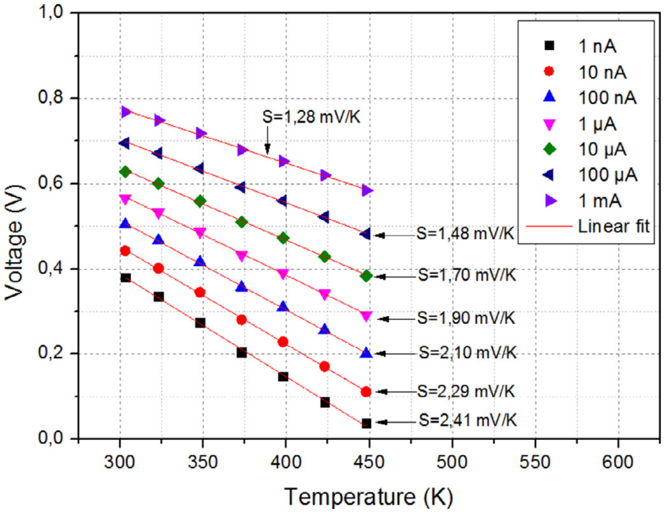

Fig. 7. V_D–T data and relative best linear fit.

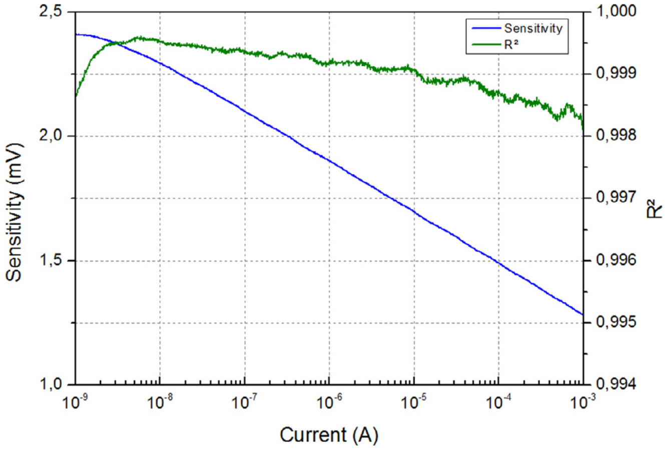

Fig. 8. Diode sensitivity (S) and relative coefficient of determination (R^2).

4. Conclusion

In this work we have simulated the I_D-V_D-T characteristics of a W/4H-SiC SBD to study the effect of temperature on the main device electrical parameters. By fitting the experimental results in the 303–448 K temperature range, we found an increase of the barrier height and a decrease of the ideality factor with temperature. The origin of these behaviors has been explained on the basis of the thermionic emission mechanism with a single Gaussian distribution of the barrier heights at the 4H–SiC interface. The obtained results in terms of S and R^2 suggest the use of the proposed device as temperature sensor.

Declaration of Competing Interest

The authors declare that they have no known competing financial interests or personal relationships that could have appeared to influence the work reported in this paper.

CRediT authorship contribution statement

Kamal Zeghdar: Methodology, Investigation, Writing - original draft. **Hichem Bencherif:** Software, Data curation, Formal analysis. **Lakhdar Dehimi:** Conceptualization, Supervision, Writing - review & editing. **Fortunato Pezzimenti:** Methodology, Supervision, Writing - review & editing. **Francesco G. DellaCorte:** Conceptualization, Visualization, Supervision.

References

[1] K. Zeghdar, L. Dehimi, F. Pezzimenti, M.L. Megherbi, F.G. Della Corte, Analysis of the electrical characteristics of Mo/4H-SiC Schottky barrier diodes for temperature-sensing applications, J. Electron. Mater. 49 (2020) 1322–1329, doi:10.1007/s11664-019-07802-6.

[2] S. Rao, G. Pangallo, F. Pezzimenti, F.G. Della Corte, High-performance temperature sensor based on 4H-SiC Schottky diodes, IEEE Electron. Dev. Lett. 36 (2015) 720–722, doi:10.1109/LED.2015.2436213.

[3] K. Zekentes, K. Vasilevskiy, Advancing silicon carbide electronics technology i: metal contacts to silicon carbide: physics, technology, applications, Mater. Res. Forum LLC (2018).

[4] S. Toumi, A. Ferhat-Hamida, L. Boussouar, A. Sellai, Z. Ouennoughi, H. Ryssel, Gaussian distribution of inhomogeneous barrier height in tungsten/4H- SiC (000-1) Schottky diodes, Microelectron. Eng. 86 (2009) 303–309, doi:10.1016/j.mee.2008.10.015.

[5] Silvaco Atlas User's Manual, Device Simulator Software, 2013.

[6] S. Selberherr, Analysis and Simulation of Semiconductor Devices, Springer Science & Business Media, 1984, doi:10.1007/978-3-7091-8752-4_4.

[7] A. Galeckas, J. Linnros, V. Grivickas, U. Lindefelt, C. Hallin, Auger recombination in 4H-SiC: unusual temperature behavior, Appl. Phys. Lett. 71 (1997) 3269–3271, doi:10.1063/1.120309.

[8] U. Lindefelt, Doping-induced band edge displacements and band gap narrowing in 3C–, 4H–, 6H–SiC, and Si, J. Appl. Phys. 84 (2019) 2628–2637, doi:10.1063/1.368374.

[9] X. Li, Y. Luo, L. Fursin, J.H. Zhao, M. Pan, P. Alexandrov, M. Wein, On the temperature coefficient of 4H-SiC BJT current gain, Solid State Electron. 47 (2003) 233–239, doi:10.1016/s0038-1101(02)00200-9.

[10] M. Roschke, F. Schwierz, Electron mobility models for 4H, 6H, and 3C SiC [MESFETs], IEEE Trans. Electron. Devices 48 (2001) 1442–1447, doi:10.1109/16.930664.

[11] M.J. Bozack, Surface studies on SiC as related to contacts, Phys. Status Solidi 202 (1997) 549, doi:10.1002/1521-3951(199707)202:1⟨549::aid-pssb549⟩3.0.co;2-6.

[12] K. Zeghdar, L. Dehimi, F. Pezzimenti, S. Rao, F. Della Corte, Simulation and analysis of the current–voltage–temperature characteristics of Al/Ti/4H-SiC Schottky barrier diodes, Jpn. J. Appl. Phys. 58 (2019) 014002, doi:10.7567/1347-4065/aaf3ab.

[13] A. Fritah, L. Dehimi, F. Pezzimenti, A. Saadoune, B. Abay, Analysis of I–V– T characteristics of Au/n-InP schottky barrier diodes with modeling of nanometer-sized patches at low temperature, J. Electron Mater. 48 (2019) 3692–3698, doi:10.1007/s11664-019-07129-2.

[14] R. Tung, Electron transport at metal-semiconductor interfaces: general theory, Phys. Rev. B 45 (1992) 13509–13523, doi:10.1103/PhysRevB.45.13509.

[15] J. Sullivan, R. Tung, M. Pinto, W. Graham, Electron transport of inhomogeneous Schottky barriers: a numerical study, J. Appl. Phys. 70 (1991) 7403–7424, doi:10.1063/1.349737.

[16] J. Werner, H. Güttler, Barrier inhomogeneities at Schottky contacts, J. Appl. Phys. 69 (1991) 1522–1533, doi:10.1063/1.347243.